01 Sep 2022

# A Heuristic Approach to Predict the Tensile Strength of a Non-Persistent Jointed Brazilian Disc under Diametral Loading

Mostafa Asadizadeh

Nima Babanouri

Taghi Sherizadeh
*Missouri University of Science and Technology*, sherizadeh@mst.edu



## Recommended Citation

M. Asadizadeh et al., "A Heuristic Approach to Predict the Tensile Strength of a Non-Persistent Jointed Brazilian Disc under Diametral Loading," *Bulletin of Engineering Geology and the Environment*, vol. 81, no. 9, article no. 364, Springer, Sep 2022.
The definitive version is available at https://doi.org/10.1007/s10064-022-02869-8

Bulletin of Engineering Geology and the Environment (2022) 81: 364
https://doi.org/10.1007/s10064-022-02869-8

ORIGINAL PAPER

# A heuristic approach to predict the tensile strength of a non-persistent jointed Brazilian disc under diametral loading

**Mostafa Asadizadeh**[1] · **Nima Babanouri**[2] · **Taghi Sherizadeh**[3]

Received: 17 January 2022 / Accepted: 9 August 2022 / Published online: 16 August 2022


## Abstract

The mechanical response of rock bridges plays a key role in the stability of concrete and rock structures. In particular, the tensile failure of non-persistent discontinuities can result in their coalescence and the failure of rock or concrete engineering structures. The effect of non-persistent joint parameters on rock structures' failure under tensile mode has not been investigated by many researchers yet. Many non-persistent jointed Brazilian concrete discs are tested under diametral loading in this work, to study the influence of joint spacing, joint continuity factor, loading direction with regard to joint angle, and bridge angle on their tensile behavior. Heuristic methods like artificial neural network (ANN), adaptive neuro-fuzzy inference system (ANFIS) and a combination of ANFIS with particle swarm optimization (ANN-PSO) and genetic algorithm (ANFIS-GA) were adopted to explore the relationship between tensile strength and stiffness as the response and non-persistent joint parameters as input parameters. The results revealed that all the applied intelligent methods have the ability to predict tensile strength of non-persistent jointed discs, and their outputs are consistent with laboratory results; however, the ANN approach had the best performance with $R^2 = 0.966$, RMSE = 0.176. In addition, parametric analysis of the proposed model showed that the model is highly sensitive to joint continuity factor and loading direction, while it is sensitive to joint spacing and bridge angle.

**Keywords** Non-persistent joint · Brazilian Disc · Tensile strength · ANN · ANFIS

## Nomenclatures

| | |
|---|---|
| $d$ | Joint spacing (cm) |
| $\gamma$ | Bridge angle (degree) |
| $\beta$ | Loading direction with respect to joint angle (degree) |
| $L_j$ | Joint length (cm) |
| $L_j$ | Rock bridge length (cm) |
| $k$ | Joint continuity factor ($k = \frac{L_j}{L_j+L_r}$) |
| $\sigma_1$ | Major principal stress |
| UCS | Unconfined compressive strength |
| $E$ | Young's modulus (GPa) |
| $\sigma_t$ | Tensile strength (MPa) |
| $\nu$ | Poisson's ratio |
| *MPSA* | Multiple parametric sensitivity analysis |
| $f_h$ | Objective Function |
| $\delta_h$ | Independent relative importance of each parameter |
| $\boldsymbol{\gamma}$ | Sum of independent relative importance of each parameter |
| *ANN* | Artificial neural network |
| *ANFIS* | Adaptive neuro-fuzzy inference system |
| *PSO* | Particle swarm optimization |
| *GA* | Genetic algorithm |

✉ Mostafa Asadizadeh
masadizadeh@mines.edu

[1] Colorado School of Mines, 1500 Illinois St., Golden, CO 80401, USA

[2] Department of Mining Engineering, Hamedan University of Technology, Mardom Street, Hamedan 65155-579, Iran

[3] Department of Mining and Nuclear Engineering, Missouri, University of Science and Technology, Rolla, MT 65409, USA

## Introduction

Rock blocks and discontinuities, like joints, bedding planes and faults, are two main components of any rock masses. The stability of rock structures depends on both the properties of intact rock and rock discontinuities (Wittke 2014). Discontinues in rock mass can be divided into persistent or non-persistent one, and they may affect the mechanical behavior of rock mass (Jennings 1970; Lajtai 1973). A large number of rock engineering structures, such as slopes, mines, and

tunnels, may contain non-persistent joints (Bahaaddini et al. 2016; Azarfar et al. 2018; Vaziri et al. 2022). The tensile strength of rock bridges is an important factor controlling the mechanical response of rock masses (Bahaaddini et al. 2013; Asadizadeh et al. 2018a, b, 2019; Karimi et al. 2021; Shakeri et al. 2022). Therefore, an in-depth knowledge of the crack development in rock mass is essential for the assessment and design of the stability of rock structures. Since in situ studding of rock mass cracking behavior is difficult, a vast number of studies have been conducted on natural or rock-like material containing pre-fabricated joints, and many outstanding results have been reported (Asadizadeh et al. 2018a, b, 2019; Rezaei and Asadizadeh 2020; Karimi et al. 2021; Shakeri et al. 2022). Much research has been conducted to study the mechanical response of persistent joints (Barton 1973; Wang and Huang 2009; Asadizadeh et al. 2010) and less to study the non-persistent joints (Bahaaddini et al. 2013; Yang et al. 2016; Asadizadeh et al. 2018b, 2019; Shakeri et al. 2022). However, tensile behavior of samples containing non-persistent joints has not been explored thoroughly yet (Cheng et al. 2016; Shang et al. 2018; Lin et al. 2020; Yang et al. 2020).

With the advent of high-speed computers, artificial intelligent approaches have been adopted to explore the complexity of geotechnical problems (Sharbati et al. 2022; Tsuruta et al. 2019; Asadizadeh and Majdi 2019; Rivera and Bonilla 2020; Rezaei and Asadizadeh 2020; Mahmoodzadeh et al. 2021). These methods have been used to explore rock engineering problems in both mining and civil engineering disciplines (Asadizadeh and Hossaini 2016; Haeri et al. 2016; Asadizadeh and Majdi 2019; Luo et al. 2021; Lawal and Kwon 2021). Adopted Mamdani fuzzy system to predict the deformation modulus of roof rock strata in longwall mining. They employed fuzzy logic to evaluate deformation modulus utilizing rock mass properties. In another research, predicted deformation modulus of rock mass using radial basis function neural network (RBFNN) based on in situ dilatometer tests, and they reported excellent performance for RBFNN to predict deformation modulus. Haeri et al. (2016) investigated crack coalescence in concrete utilizing the ANN approach. The model performance was evaluated, and the results were compared to those obtained using the experimental technique, and the results revealed the capability of artificial neural networks to predict failure mode in concrete samples. Sarfarazi et al. (2020) used experimental testing and numerical modeling to investigate the tensile behavior of a Y-shaped non-persistent junction. The results revealed that the minimum tensile strength occurs at a 60° angle between the bigger joint and the horizontal axis and that increasing the notch length decreased the tensile strength. Both approaches indicated identical failure patterns and failure strengths. Employed a neuro-fuzzy model, which was developed by artificial bee colony techniques to assess the rock brittleness index. Tensile behavior of rock mass including non-persistent joints subjected to static loads has been studied by few researchers using artificial intelligent approaches (Feng et al. 2018; Nguyen et al. 2020).The tensile strength of intermittent joints and intact rock bridges is not well explored, and more investigations are needed to boost the knowledge. These studies are beneficial to engineers by giving them a better understanding of how rock structures fail when subjected to static loads in situations like slopes, tunnels, and underground spaces and by assisting their stability during the design stage and preventing catastrophic failures.

In this paper, through physical experiments and heuristic approaches, many Brazilian concrete discs, including a number of non-persistent joints, are under diametral loading to study the impact of bridge angle, joint spacing, loading direction with respect to the joint angle, and joint continuity factor (see Fig. 1). Several intelligent techniques including ANN, ANFIS and ANN-PSO/GA have been applied to the experimental data to predict the tensile strength $(\sigma_t)$ of the samples, and the performance of artificial intelligent approaches was evaluated using several statistical indicators.

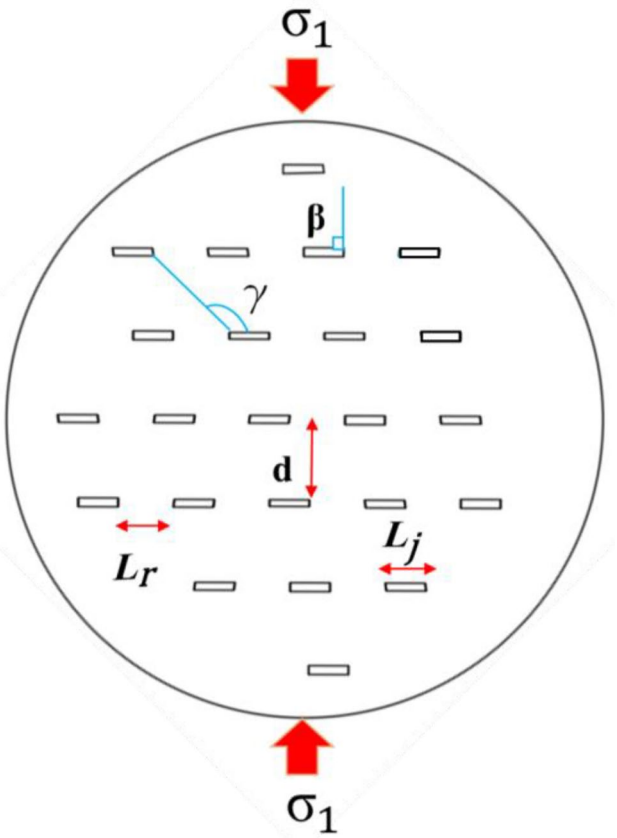


**Fig.1** Non-persistent jointed discs' geometric parameters

**Table 1** Brazilian concrete discs' material properties

| $\sigma_t$ (MPa) | UCS (MPa) | $E$ (GPa) | $\nu$ |
|---|---|---|---|
| 1.88 | 12.96 | 2.44 | 0.25 |

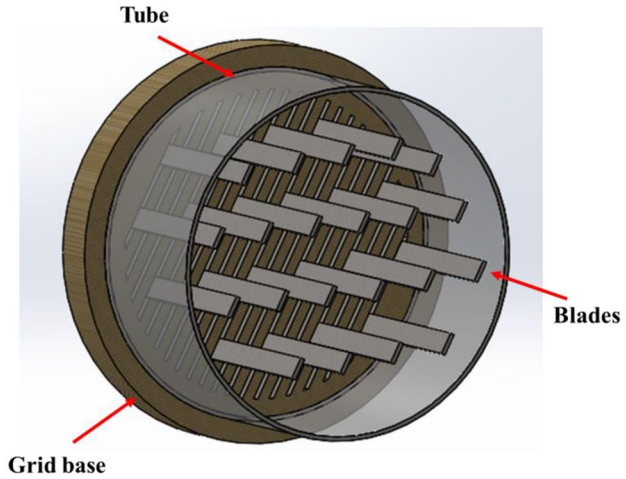


**Fig. 2** A view of a plexiglass mold

## Experimental program

Concrete Brazilian disc samples (diameter = 150 mm, height = 75 mm) were made with a 3.5:5:3 weight ratio of cement, sand, and water. The samples were submerged for 14 days at room temperature to be cured. On cylindrical and disc specimens, some uniaxial compression and Brazilian tests were conducted to determine their mechanical properties. Table 1 shows the mechanical parameters of the final product. A geologic material with the described mechanical qualities is classified as a weak rock sample.

According to (Brady and Brown 2004), plexiglass and PVC tube were used to design and produce a specific mold. A grid of slots was created to provide a host for the blades which are installed vertically at the bottom of the model. The blades were fixed at the bottom of model using a predesigned grid. A view of mold setup is shown in Fig. 2.

To free the air bubble in the mortar, it was shaken for 2 min, and after four hours the blades were smoothly removed from the mortar to generate the non-persistent joints in the model. A view of model before and after testing is shown in Fig. 3.

### Testing procedure

Uniaxial loading setup available in the rock mechanics laboratory of Hamadan University of Technology was used to apply diametral load to the non-persistent jointed Brazilian disc (Bieniawski and Hawkes 1978). To achieve this goal, 72 Brazilian disc samples were created and tested. The specimen was subjected to an axial displacement rate equal to 0.005 mm/s. Furthermore, the LVDT displacement sensor was utilized in this experiment to study and calculate the values of stress and strain, which is shown in Fig. 4, a view of the uniaxial loading setup and how the samples are placed under loading. Note that in this article, all experiments were performed on 14-day-old samples.

### Experimental program

The effect of four parameters including $k$, $d$, $\gamma$ and $\beta$ on the tensile behavior of non-persistent jointed discs has been studied (Fig. 1). The input and output parameters of experiments are presented in Table 2.

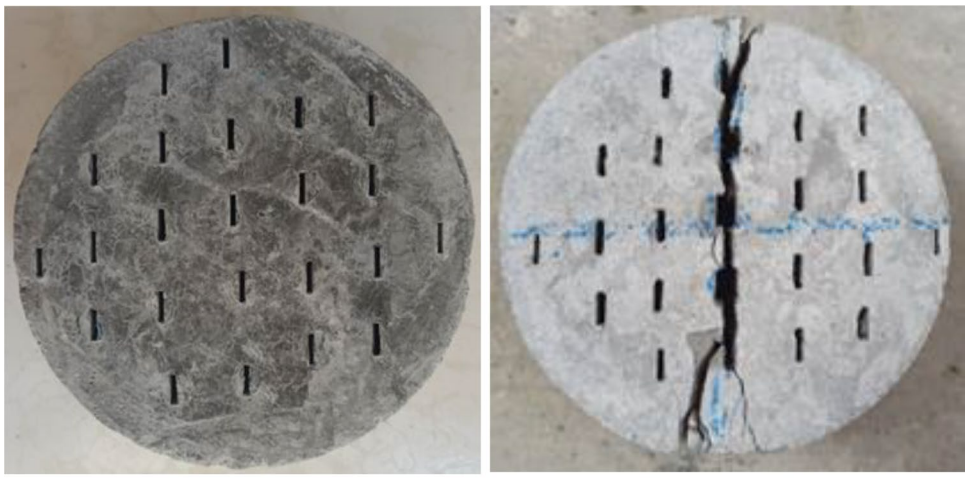


**Fig. 3** **a** Before and **b** after the test of a Brazilian concrete disc sample

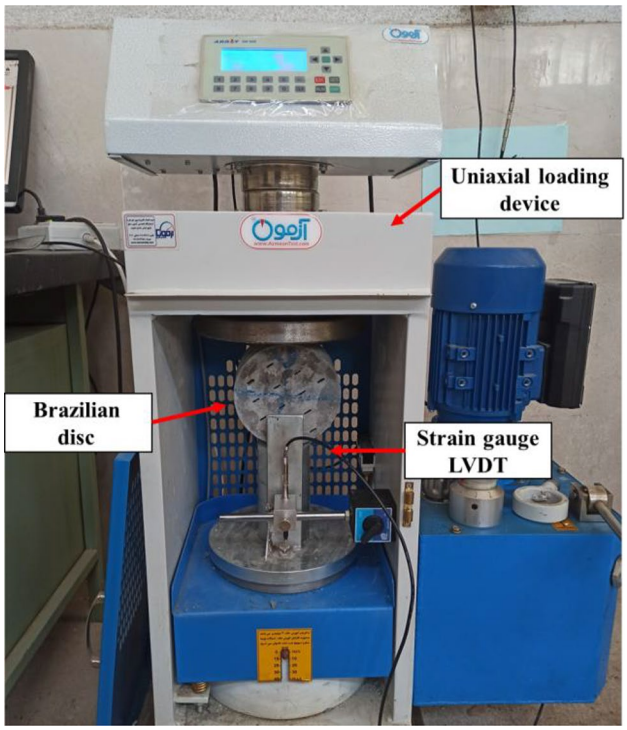


**Fig. 4** A view of the uniaxial loading configuration

## Applied methods

In this research in order to explore the tensile behavior of samples, four heuristic approaches have been adopted. Each method is shortly explained in the following sections.

*PSO* Particle Swarm Optimization.

### Artificial neural network

ANNs are widely recognized as one of the most effective and widely used prediction systems. ANNs have been used in a number of studies to investigate rock engineering issues (Rezaei 2017, 2019). Any ANN model consists of input, hidden and output layers (Rajabi et al. 2017). One of the most prevalent varieties of ANN is the multilayer perceptron (MLP), which consists of a series of layers connected by neurons. The most important parts of multilayer networks include non-trivial calculation, learning, and generalization. The number of neurons is determined by the problem's complexity and the nature of the data. The hidden layers, which are located in the middle, are not directly connected to the input or output data (Rezaei 2016). MLP transforms Xn inputs into outputs using nonlinear operators (Shojaeian and Asadizadeh 2020; Rezaei and Asadizadeh 2020). The literature contains in-depth information about MLP (Armaghani et al. 2015; Rezaei 2019). A view of MLP ANN with a hidden layer is shown in Fig. 5.

### Adaptive neuro-fuzzy inference system

A feed-forward ANN, which uses fuzzy logic to find the best layer weights, converts inputs to outputs is called adaptive neuro-fuzzy inference system (ANFIS) and was introduced by Jang 1993. This algorithm is basically adopted for training purposes to tune the Sugeno-FIS parameters in order to find the best relation between input and output parameters with the minimum error.

As a learning algorithm, ANFIS employs the gradient descent and the least squares estimate approaches (Saberi et al. 2022). The initial input–output pairs have been generated using a group of fuzzy "If–Then" rules with appropriate membership functions. Some nodes with specific functions, which are organized in layers, may generate a network. Lensing phase involves input variables propagating and applying least mean square in an iterative way to evaluate the optimized parameters and then follows by pattern repetition adopting propagation algorithm to tune the ancestor parameters (Asadizadeh and Majdi 2019; Shojaeian and Asadizadeh 2020). Figure 6 depicts the ANFIS system's structure. The ANFIS is made up of a neural network with five layers: input nodes are in the first layer, nodes of membership rules or functions are in second the layer, first segment of fuzzy rules to explore the ratio of normalized rules is located in the third layer, as shown in this diagram. The fourth layer comprises the fuzzy rules' result nodes, whereas the fifth layer is the fuzzy decoupling phase, or output node, which explore the final response as the sum of all the input variables (Jang 1993).

### Particle swarm optimization

PSO is a metaheuristic and population-based technique that uses an optimization process to iteratively search for a better viable solution (Huang et al. 2020). Particles go forward through a search space with multidimension to locate the optimal solution in this method. As a result, many particles should be formed and scattered in the search space in each optimization problem (Hajihassani et al. 2015). The fundamental disadvantage of PSO is its sluggish convergence, although it is ideal for finding local extremums (Victoire and Jeyakumar 2004). In the search space, the location of the particles changes depending on their history and the position of their neighboring particles. The particles would generate a population, which is referred to as a swarm in the literature. Figure 7 depicts the PSO algorithm's basic flow.

### Genetic algorithm

The GA is a search algorithm and stochastic optimization approach invented by (Holland 1992). This approach was developed based on biological species evolution

**Table 2** Tensile strength predictions are based on all available data

| Sample cod | $k$ | $d$ (cm) | $\gamma$ (°) | $B$ (°) | $(\sigma_t)$(MPa) | Sample cod | $k$ | $d$ (cm) | $\gamma$ (°) | $\beta$ (°) | $(\sigma_t)$(MPa) |
|---|---|---|---|---|---|---|---|---|---|---|---|
| S1 | 0.67 | 2.8 | 121.5 | 45 | 1 | S37 | 0.29 | 2.8 | 121.5 | 45 | 1.61 |
| S2 | 0.67 | 2.8 | 121.5 | 45 | 0.56 | S38 | 0.29 | 2.8 | 121.5 | 45 | 1.67 |
| S3 | 0.67 | 2.8 | 121.5 | 45 | 1.33 | S39 | 0.29 | 2.8 | 121.5 | 45 | 1.67 |
| S4 | 0.4 | 2.8 | 121.5 | 45 | 1.72 | S40 | 0.29 | 2.8 | 130.5 | 45 | 2 |
| S5 | 0.4 | 2.8 | 121.5 | 45 | 1.61 | S41 | 0.29 | 2.8 | 130.5 | 45 | 2.05 |
| S6 | 0.4 | 2.8 | 121.5 | 45 | 1.61 | S42 | 0.29 | 2.8 | 130.5 | 45 | 1.67 |
| S7 | 0.29 | 2.8 | 121.5 | 45 | 1.67 | S43 | 0.29 | 2.8 | 150 | 45 | 1.67 |
| S8 | 0.29 | 2.8 | 121.5 | 45 | 1.72 | S44 | 0.29 | 2.8 | 150 | 45 | 1.67 |
| S9 | 0.29 | 2.8 | 121.5 | 45 | 1.72 | S45 | 0.29 | 2.8 | 150 | 45 | 1.72 |
| S10 | 0.22 | 2.8 | 121.5 | 45 | 1.83 | S46 | 0.29 | 1.4 | 121.5 | 45 | 1.5 |
| S11 | 0.22 | 2.8 | 121.5 | 45 | 2.05 | S47 | 0.29 | 1.4 | 121.5 | 45 | 1.72 |
| S12 | 0.22 | 2.8 | 121.5 | 45 | 2.28 | S48 | 0.29 | 1.4 | 121.5 | 45 | 1.5 |
| S13 | 0.18 | 2.8 | 121.5 | 45 | 1.72 | S49 | 0.29 | 2.1 | 121.5 | 45 | 1.67 |
| S14 | 0.18 | 2.8 | 121.5 | 45 | 1.72 | S50 | 0.29 | 2.1 | 121.5 | 45 | 1.5 |
| S15 | 0.18 | 2.8 | 121.5 | 45 | 1.5 | S51 | 0.29 | 2.1 | 121.5 | 45 | 1.61 |
| S16 | 0.29 | 2.8 | 121.5 | 0 | 1.72 | S52 | 0.29 | 2.8 | 121.5 | 45 | 1.78 |
| S17 | 0.29 | 2.8 | 121.5 | 0 | 1.61 | S53 | 0.29 | 2.8 | 121.5 | 45 | 1.5 |
| S18 | 0.29 | 2.8 | 121.5 | 0 | 1.89 | S54 | 0.29 | 2.8 | 121.5 | 45 | 1.5 |
| S19 | 0.29 | 2.8 | 121.5 | 20 | 1.72 | S55 | 0.29 | 3.5 | 121.5 | 45 | 1.89 |
| S20 | 0.29 | 2.8 | 121.5 | 20 | 1.33 | S56 | 0.29 | 3.5 | 121.5 | 45 | 1.5 |
| S21 | 0.29 | 2.8 | 121.5 | 20 | 1.89 | S57 | 0.29 | 3.5 | 121.5 | 45 | 1.17 |
| S22 | 0.29 | 2.8 | 121.5 | 45 | 1.44 | S58 | 0.29 | 4.2 | 121.5 | 45 | 1.83 |
| S23 | 0.29 | 2.8 | 121.5 | 45 | 1.17 | S59 | 0.29 | 4.2 | 121.5 | 45 | 1.83 |
| S24 | 0.29 | 2.8 | 121.5 | 45 | 1.44 | S60 | 0.29 | 4.2 | 121.5 | 45 | 1.89 |
| S25 | 0.29 | 2.8 | 121.5 | 70 | 1.83 | S61 | 0.67 | 2.1 | 135 | 45 | 1.22 |
| S26 | 0.29 | 2.8 | 121.5 | 70 | 1.55 | S62 | 0.67 | 2.1 | 135 | 45 | 1.33 |
| S27 | 0.29 | 2.8 | 121.5 | 70 | 1.89 | S63 | 0.67 | 2.1 | 135 | 45 | 0.94 |
| S28 | 0.29 | 2.8 | 121.5 | 90 | 1.11 | S64 | 0.42 | 2.1 | 135 | 90 | 0.83 |
| S29 | 0.29 | 2.8 | 121.5 | 90 | 1.11 | S65 | 0.42 | 2.1 | 135 | 90 | 0.78 |
| S30 | 0.29 | 2.8 | 121.5 | 90 | 1 | S66 | 0.42 | 2.1 | 135 | 90 | 0.56 |
| S31 | 0.29 | 2.8 | 90 | 45 | 1.61 | S67 | 0.42 | 2.8 | 135 | 45 | 0.83 |
| S32 | 0.29 | 2.8 | 90 | 45 | 1.67 | S68 | 0.42 | 2.8 | 135 | 45 | 1.17 |
| S33 | 0.29 | 2.8 | 90 | 45 | 1.55 | S69 | 0.42 | 2.8 | 135 | 45 | 0.89 |
| S34 | 0.29 | 2.8 | 112.5 | 45 | 1.83 | S70 | 0.17 | 2.1 | 135 | 45 | 1 |
| S35 | 0.29 | 2.8 | 112.5 | 45 | 1.89 | S71 | 0.17 | 2.1 | 135 | 45 | 1.28 |
| S36 | 0.29 | 2.8 | 112.5 | 45 | 1.83 | S72 | 0.17 | 2.1 | 135 | 45 | 1.39 |

and natural selection mechanism, and it has been widely adopted to solve optimization problems. The GA, which belongs to a broad category of evolutionary algorithms (EA), can solve optimization problems by employing strategies based on natural evolution ideas including inheritance, mutation, selection and crossover (Martin et al. 2011). As shown in Fig. 8, the algorithm begins with the beginning population, and the optimal size of the population is determined by the problem's complexity (Höglund 2017). The chromosomes produced by chance as the first-generation size (starting population) are determined. A roulette wheel is used to pick the major chromosomes for the manufacturing process.

Two chromosomes will join together to produce two new ones using a cross-mechanism. It is then chosen and repeated until a new generation of children is produced. Crossover is the next step in the manufacturing process, and it involves a genetic algorithm combining genetic data from two parents to make new children (Shojaeian and Asadizadeh 2020). The mutation rate is another important element in the genetic algorithm, which is employed to keep genetic truth from one chromosomal generation to the next. The mutation process can modify the values of one or more genes on a chromosome. The fitness function for the chromosomes is tested when the new population is generated, and the selection process begins. After that, the

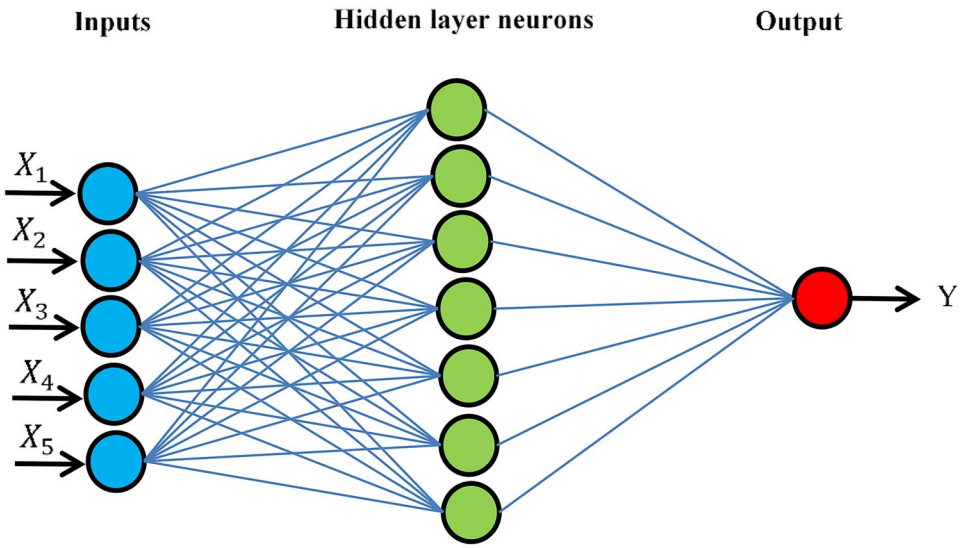


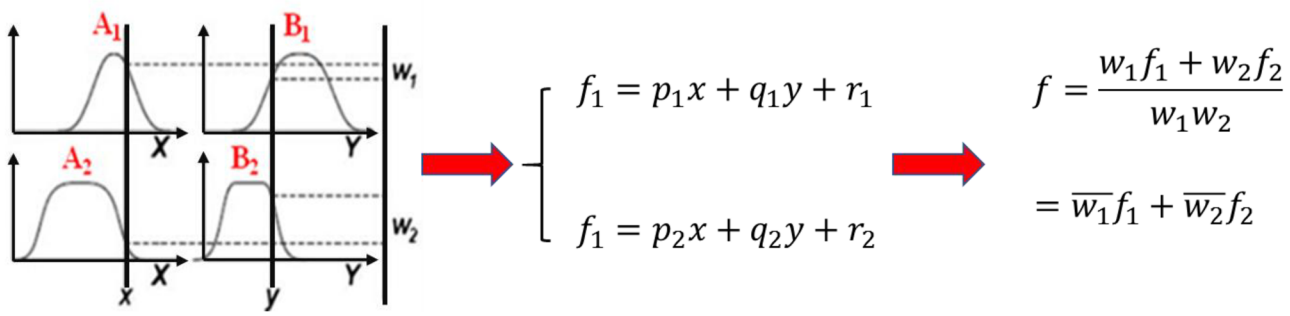


**(a)**

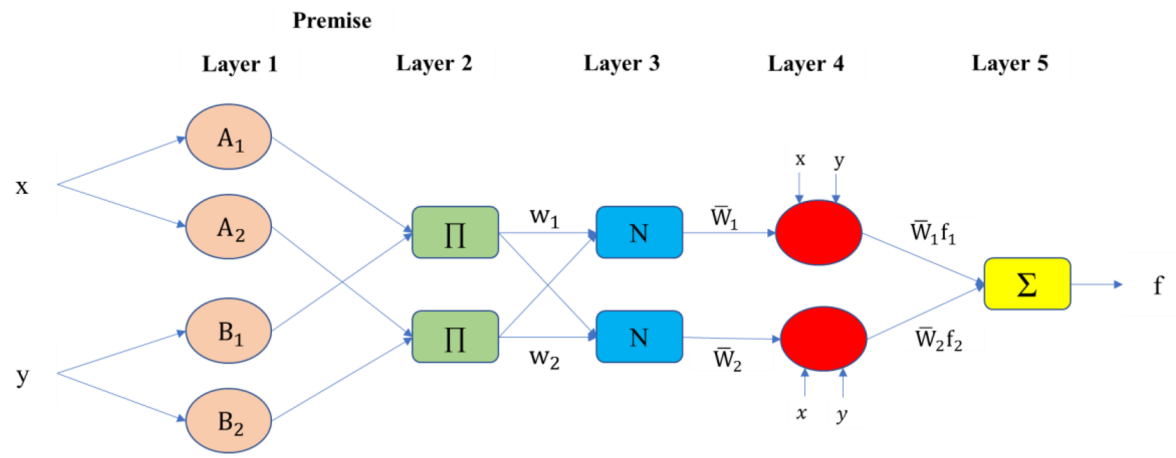


**(b)**

**Fig. 5** MLP ANN with a hidden layer (Shojaeian and Asadizadeh 2020)

**Fig. 6** **a** Fuzzy inference; **b** equivalent infinity structure (Jang 1993)

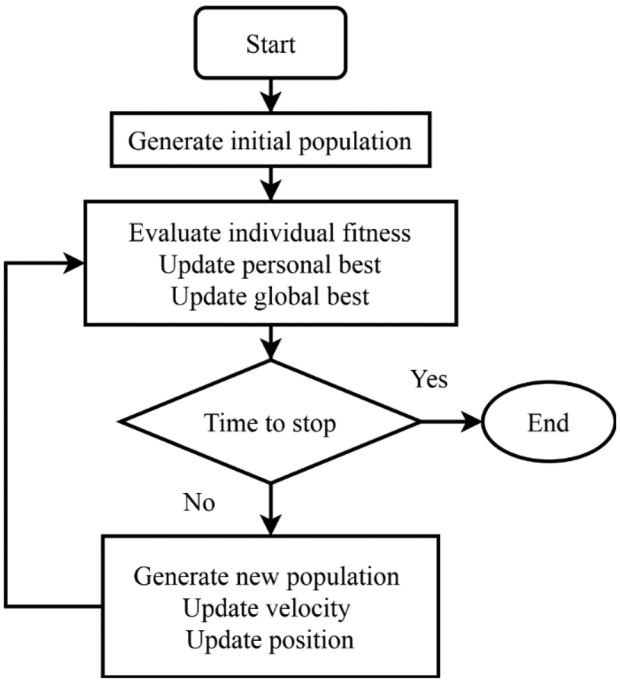


**Fig. 7** The particle swarm's flow diagram (Aydin et al. 2013)

evolutionary process continues until the best solution to the problem is found (Momeni et al. 2014).

## Database

Input variables play an important role in creating a successful forecasting model. To select the effective parameters in predicting the amount of tensile strength, based on "expert opinions", four input parameters shown in Table 3 are considered.

The total number of data is 73. In all models, 70% of the data was used randomly for training and 30% of the data was used for model validation and testing. An in-depth statistical analysis of data was performed, and the histogram of input and output data is shown in Fig. 9.

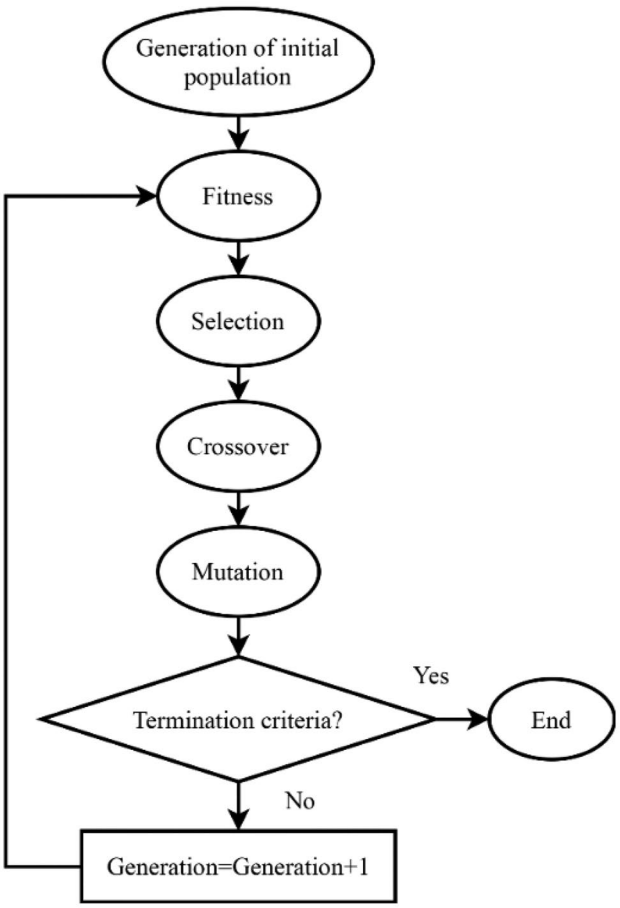


**Fig. 8** GA flowchart in its simplest form (Martin et al. 2011)

## Result and discussion

### ANN approach

By having adequate data for model training phase and using the appropriate training method, the ANN is able to learn the sophisticated relationships between inputs and outputs well. In this study, a multilayer network of perceptron known as MLP-ANN was adopted to estimate the amount of the tensile

**Table 3** Parameters for model's input and output.

| Type | Parameter | Symbol | Range | Min | Max | Mean | Std. Deviation | Variance |
|---|---|---|---|---|---|---|---|---|
| Input | Joint continuity factor | $k$ | 0.5 | 0.17 | 0.67 | 0.322 | 0.120 | 0.014 |
| | Joint spacing (cm) | $d$ | 2.8 | 1.4 | 4.2 | 2.713 | 0.511 | 0.261 |
| | Bridge angle (degree) | $\gamma$ | 60 | 90 | 150 | 123.625 | 10.455 | 109.315 |
| | Loading direction (degree) | $\beta$ | 90 | 0 | 90 | 46.880 | 17.491 | 305.942 |
| Output | Tensile strength (MPa) | $\sigma_t$ | 1.72 | 0.56 | 2.28 | 1.520 | 0.362 | 0.131 |

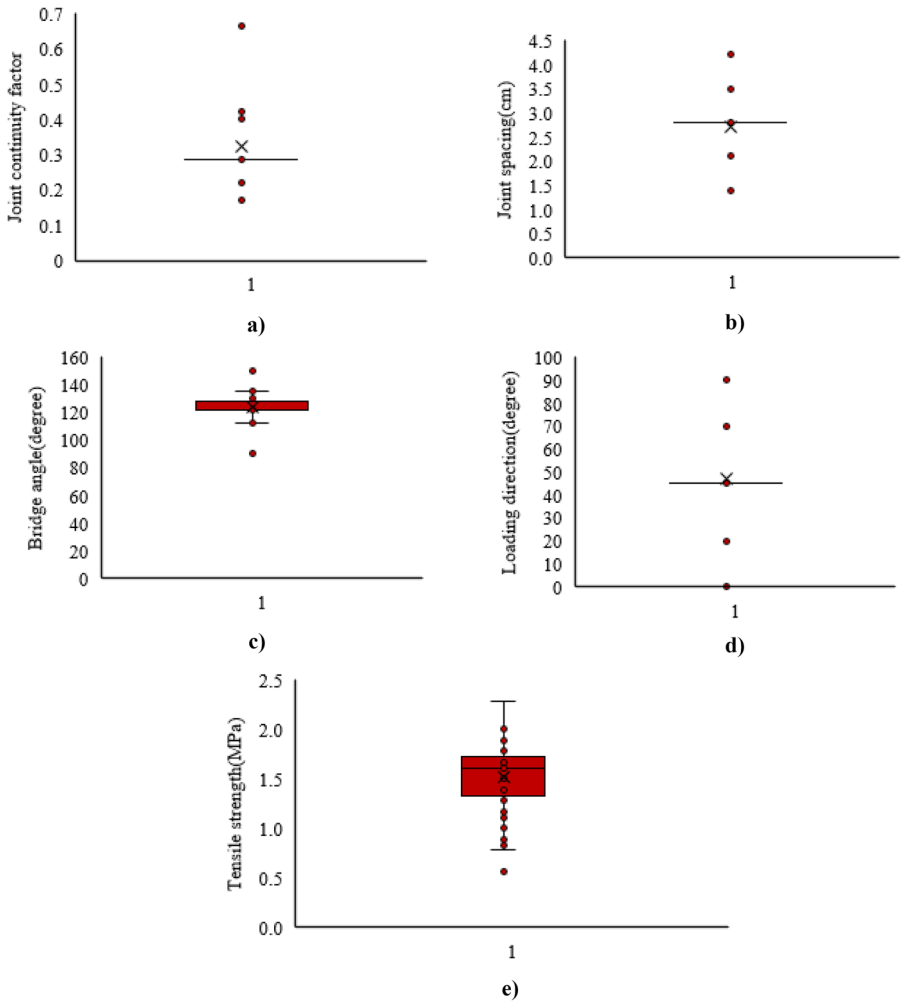


**Fig. 9** Input and output data box diagram: **a** joint continuity factor, **b** joint spacing (cm), **c** bridge angle (degree), **d** loading direction (degree), **e** tensile strength (MPa)

strength of the samples. Several neural network models were investigated to fulfill this goal, and the best models are listed in Table 4. As previously said, the data are divided into three categories: educational data, validation data, and test

**Table 4** Information of neural network parameters for tensile strength $(\sigma_t)$ prediction

| ANN Parameters | model |
|---|---|
| Input neurons | 7 |
| Hidden layers | 1 |
| Hidden neurons | 12 |
| Output neurons | 1 |
| Total data | 72 |
| Train data | 50 |
| Validation data | 11 |
| Test data | 11 |
| Training epochs | 1000 |
| Optimization approach | Levenberg–Marquardt |
| Transfer function | TANSIG |
| Learning rate | 0.1 |

**Table 5** $R^2$, RMSE, MSE, MAE, VAF and CE of the ANN models for tensile strength data

| | | Models | | | |
|---|---|---|---|---|---|
| | Index | ANN1 | ANN2 | ANN3 | ANN4 |
| **Train** | $R^2$ | 0.877 | 0.890 | 0.888 | 0.851 |
| | RMSE | 0.186 | 0.163 | 0.151 | 0.17 |
| | MSE | 0.035 | 0.027 | 0.023 | 0.029 |
| | MAE | 0.141 | 0.115 | 0.114 | 0.119 |
| | VAF | 76.932 | 79.286 | 78.775 | 72.464 |
| | CE | 0.684 | 0.743 | 0.732 | 0.613 |
| **Validation** | $R^2$ | 0.787 | 0.906 | 0.849 | 0.918 |
| | RMSE | 0.172 | 0.129 | 0.24 | 0.127 |
| | MSE | 0.03 | 0.017 | 0.057 | 0.016 |
| | MAE | 0.139 | 0.106 | 0.169 | 0.108 |
| | VAF | 61.813 | 81.509 | 72.05 | 83.763 |
| | CE | 0.303 | 0.721 | 0.581 | 0.774 |
| **Test** | $R^2$ | 0.942 | 0.909 | 0.954 | 0.966 |
| | RMSE | 0.183 | 0.187 | 0.115 | 0.174 |
| | MSE | 0.033 | 0.035 | 0.013 | 0.03 |
| | MAE | 0.129 | 0.152 | 0.102 | 0.141 |
| | VAF | 70.217 | 82.209 | 90.93 | 89.693 |
| | CE | 0.786 | 0.714 | 0.904 | 0.771 |

data, with a 70, 15 and 15% ratio, respectively. The range of changes of the input and output variables of neural networks should be considered because the more the network can generalize and understand the link between these parameters, the closer the range of changes of these parameters is. The grid only deals with the numerical values of the parameters, not their measurement units. Furthermore, the number of concealed neurons was determined by a trial-and-error method. Table 4 shows the properties of the trained network for the best ANN model.

In a regression model, R-squared (R^2) is a statistical measure of fit that shows how much variance in a dependent variable is explained by the independent variable(s). The standard deviation of prediction errors or residuals is referred to as the root-mean-square error (RMSE). It shows how widely the data are dispersed around the line of greatest fit. The mean of absolute error (MAE) is a statistic that assesses the average magnitude of errors in a group of forecasts without taking into account their direction. It assesses the precision of continuous variables. In other words, the MAE is the average of the absolute values of the discrepancies between the forecast and the relevant observation over the verification sample. The MAE is a linear score, which implies that in the average, all individual differences are equally weighted. Variance account for (VAF) calculates the variance between two signals. It is possible to assess the quality of quantitative estimates derived from design-based stereological approaches. This essentially means that we can gain some insight into the precision of a stereological process estimate. The coefficient of error (CE) is a metric for how accurate an estimate is. The results of using ANN to evaluate the tensile strength of the samples based on

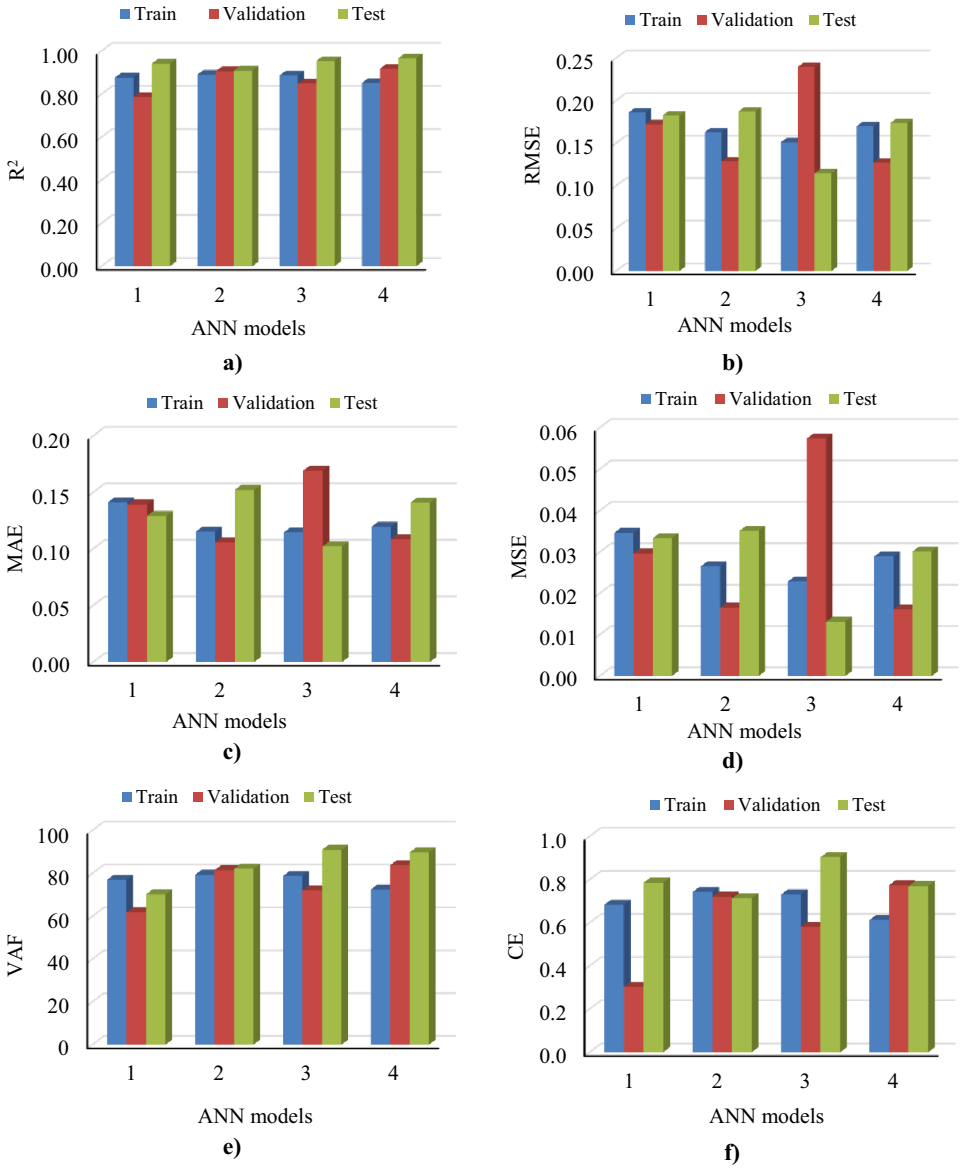


**Fig. 10** The difference between experimental tensile strength results and ANN model results. **a** $R^2$ (squared correlation coefficient), **b** RMSE (root-mean-square error), **c** MAE (mean absolute error), **d** MSE (mean square error), **e** variance account for (VAF), **f** coefficient of efficiency (CE)

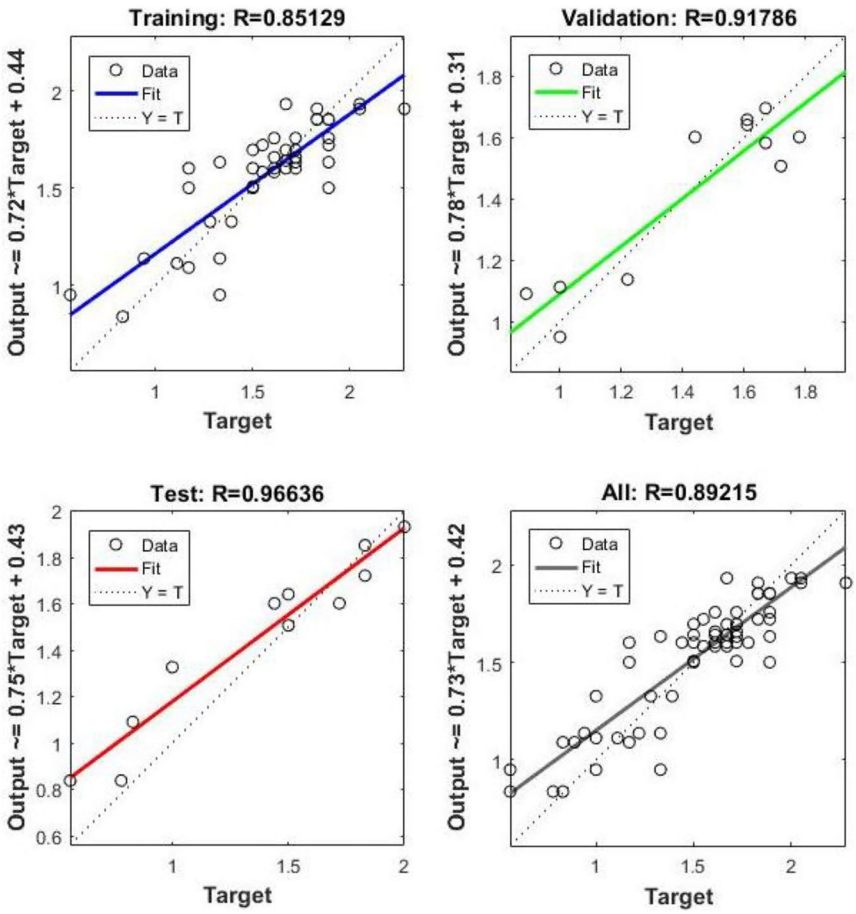


**Fig. 11** Correlation between actual and predicted tensile strength values for the best ANN model

**Table 6** The best ANFIS-/GA/PSO values

| Parameter (ANFIS) | Description/value |
|---|---|
| **Fuzzy structure** | **Sugeno-type** |
| Input membership function | Gaussian ("gaussmf") |
| Output membership function | Linear |
| The cluster influence center | 0.7 |
| No. of inputs | 4 |
| No. of outputs | 1 |
| **Optimization method** | **GA/PSO** |
| Iteration | 1000 |
| Training data | 50 |
| Test data | 22 |
| Initial step size | 0.5 |
| The decrease rate step size | 0.9 |
| The increase rate step size | 1.4 |
| Fuzzy rules | 6 |
| GA parameters | **Description/value** |
| Population size | 40 |
| Mutation rate | 0.06 |
| Crossover | 0.5 |
| PSO parameters | **Description/value** |
| Population size | 50 |
| W | 0.5 |
| C1 | 2 |
| C2 | 2 |

**Table 7** $R^2$, RMSE, MSE, MAE, VAF and CE of the ANN, ANFIS, ANFIS-GA and ANFIS-PSO models for tensile strength data

| | | Models | | | |
|---|---|---|---|---|---|
| | **Index** | **ANFIS** | **ANFIS-GA** | **ANFIS-PSO** | **ANN** |
| **Train** | **$R^2$** | 0.868 | 0.82 | 0.908 | 0.888 |
| | **RMSE** | 0.164 | 0.203 | 0.159 | 0.151 |
| | **MSE** | 0.027 | 0.041 | 0.025 | 0.023 |
| | **MAE** | 0.123 | 0.16 | 0.125 | 0.114 |
| | **VAF** | 75.356 | 67.294 | 82.423 | 78.775 |
| | **CE** | 0.673 | 0.523 | 0.785 | 0.732 |
| **Test** | **$R^2$** | 0.919 | 0.93 | 0.893 | 0.954 |
| | **RMSE** | 0.171 | 0.139 | 0.205 | 0.115 |
| | **MSE** | 0.029 | 0.019 | 0.042 | 0.013 |
| | **MAE** | 0.13 | 0.091 | 0.132 | 0.102 |
| | **VAF** | 83.831 | 86.321 | 69.099 | 90.93 |
| | **CE** | 0.765 | 0.85 | 0.712 | 0.904 |
| **All** | **$R^2$** | 0.893 | 0.875 | 0.901 | 0.921 |
| | **RMSE** | 0.168 | 0.171 | 0.182 | 0.133 |
| | **MSE** | 0.028 | 0.03 | 0.034 | 0.018 |
| | **MAE** | 0.127 | 0.125 | 0.129 | 0.108 |
| | **VAF** | 79.593 | 76.808 | 75.761 | 84.852 |
| | **CE** | 0.719 | 0.687 | 0.749 | 0.818 |

different approaches such as R^2, RMSE, MAE, VAF and CE are presented in Table 5. These studies were performed on different models of neural network, and finally, the final four models of neural network are listed in Table 5.

In order to compare the accuracy of the different methods, the outcome of the four approaches as $R^2$, RMSE, MAE, MSE, VAF and CE is shown in Fig. 10, respectively. The VAF index shows how different the variances of observed and anticipated data sets are. VAF values near 100 percent indicate reduced variability and, as a result, stronger prediction capabilities. The RMSE index is a metric for measuring the difference between measured and anticipated data. The model works better when the RMSE is low. An excellent performance is that the value of RMSE and MAE should be zero and that of CE should be one. Therefore, according to the results obtained in Fig. 10, and what was said about the indices, among the four neural network models in Table 5, model 4 is considered as the final model for predicting the amount of tensile strength.

The correlation between train, test and validation models for the final model ANN model is presented in Fig. 11.

## AAN vs. other heuristic approaches

In this section, three novel methodologies are employed to estimate the tensile strength of the samples, including ANFIS and ANFIS-GA/ PSO, and their performance is compared to the ANN method. All of the models in this

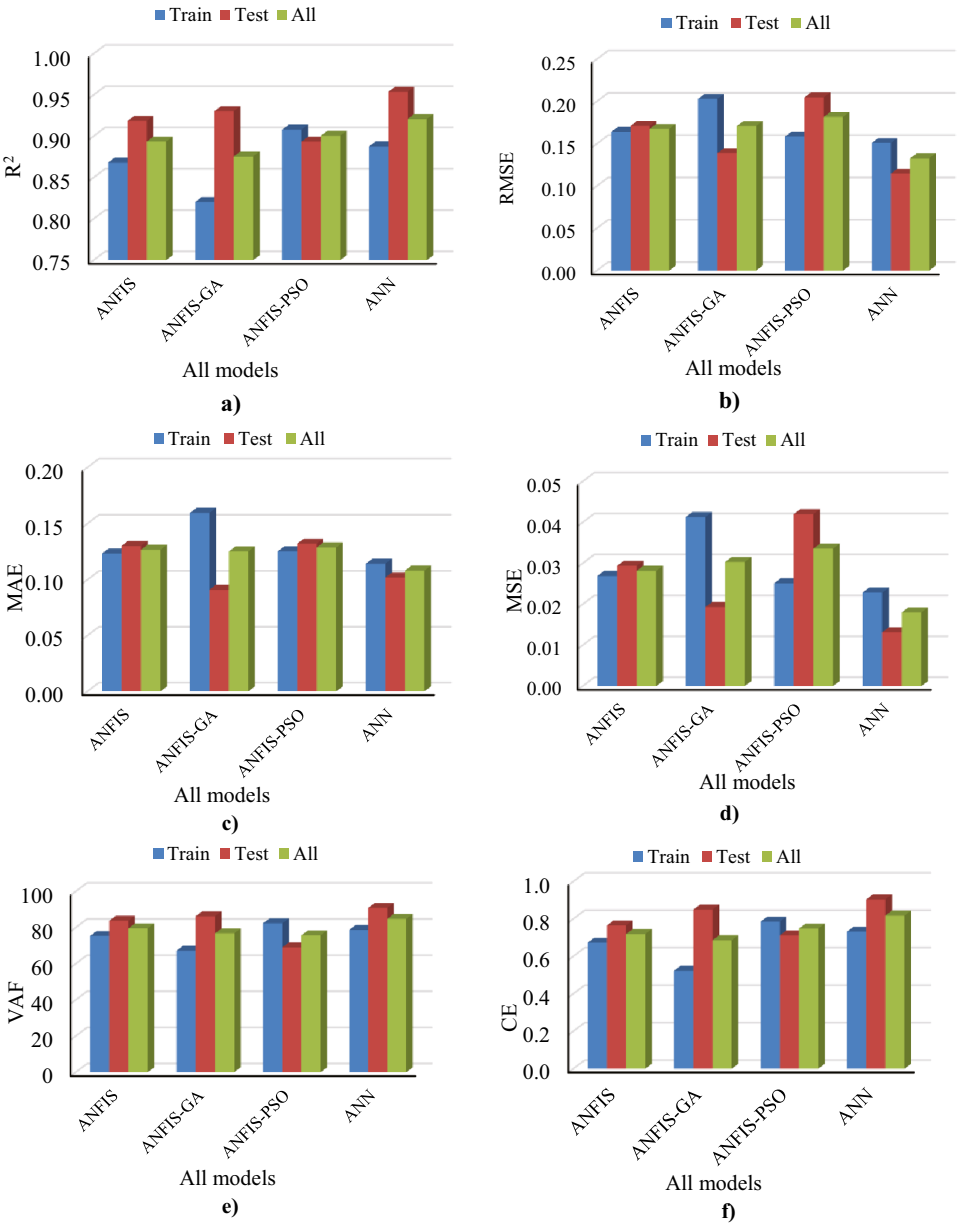


**Fig. 12** The difference in tensile strength experimental results and ANN, ANFIS, ANFIS-GA, and ANFIS-PSO model results, **a** squared correlation coefficient ($R^2$), **b** root-mean-square error (RMSE), **c** mean absolute error (MAE), **d** mean square error (MSE), **e** variance account for (VAF), **f** coefficient of efficiency (CE)

section and the previous section have the same input parameters. Learning techniques for high precision and accuracy are used individually in the ANFIS-GA/PSO method for teaching the ANFIS model. To accomplish so, GA and PSO algorithms are used to evaluate the ANFIS model's optimal parameters,GA/PSO-based. Table 6 shows the best values for the GA/PSO-based ANFIS model parameters for predicting their tensile strength.

Table 7 shows the $R^2$, MSE, RMSE, MAE, VAF and CE for train, test, and all data for the three different intelligence approaches as well as the ANN approach to forecasting tensile strength. It can be concluded that the ANN model has the best performance, followed by ANFIS-based models with nearly identical performance.

The statistical indexes of test data in Table 7 indicate that ANN has the best performance to predict tensile strength of non-persistent jointed Brazilian discs. A visual comparison between statistical parameters, which indicates the model performance, is presented in Fig. 12.

## Multiple parametric sensitivity analysis (MPSA)

The outputs of the models were subjected to a parametric analysis to determine which input factors have the greatest impact on the average output variables. The techniques shown in Fig. 13 can be used to apply MPSA to a model output for a specific set of parameters.

The objective function was evaluated using the sum of square errors between observed and modeled values:

$$f_h = \sum_{i=1}^{k} \left[x_{0,h} - x_{c,h}(i)\right]^2 \quad (1)$$

where $f_h$ is the objective function value for a particular $\sigma_t$ variable $h$; $x_{0,h}$ is the observed value at this variable; $x_{c,h}(i)$ is the computed value $x_c$ for variable $h$ for each input series; and $k$ is the number of variables contained in the random series. Table 8 shows the range of values that were utilized to evaluate each parameter. To produce 72 random numbers for each parameter, a Monte Carlo simulation was used. The trained models were given the generated numbers for one variable in each model run. Equation is used to calculate the relative relevance of each parameter separately (Correa et al. 2005):

$$\delta_h = \frac{f_h}{x_{0,h}} \quad (2)$$

Each pair of inputs is introduced by h. For each examined parameter, the results were obtained by applying the given approach to the $\sigma_t$ model. These outcomes were achieved by the application of (2). Equation 1 is used to determine the relative relevance of each parameter (Correa et al. 2005):

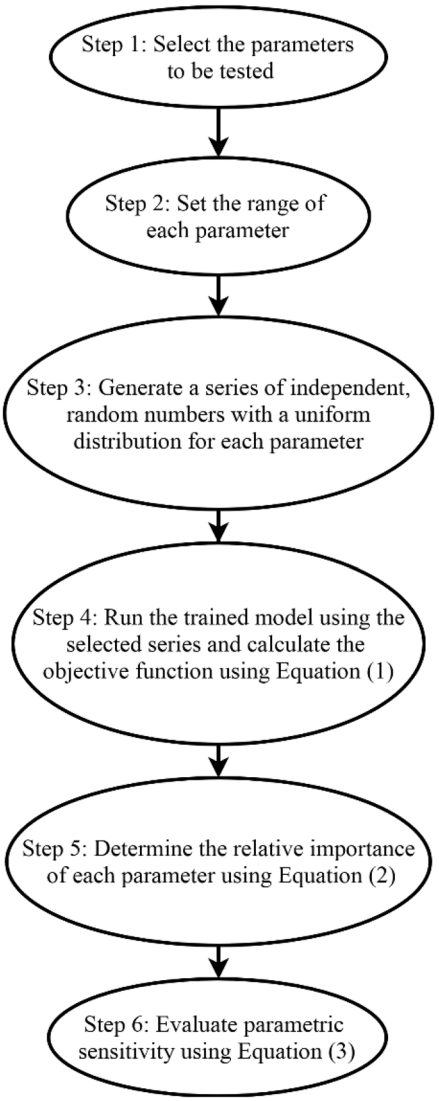


**Fig. 13** Algorithm for multiple parametric sensitivity analysis

$$\gamma = \sum_{h=1}^{i_{\sigma t,max}} \delta_h \quad (3)$$

where the $\sigma_t$ is calculated from h = 1 (the first set of data) to the maximum value $\left(i_{\sigma t,max}\right)$, for this model, which is 72 (Correa et al. 2005). The greater the $\Upsilon$ index value for each parameter, the more sensitive the $\sigma_t$ model is to that

**Table 8** The $\Upsilon$ index measures the sensitivity of model parameters (Correa et al. 2005)

| $\Upsilon$ index | Model parameter sensitivity |
|---|---|
| $\gamma \leq 1$ | Insensitive |
| $1 < \gamma \leq 100$ | Sensitive |
| $\gamma > 100$ | Highly sensitive |

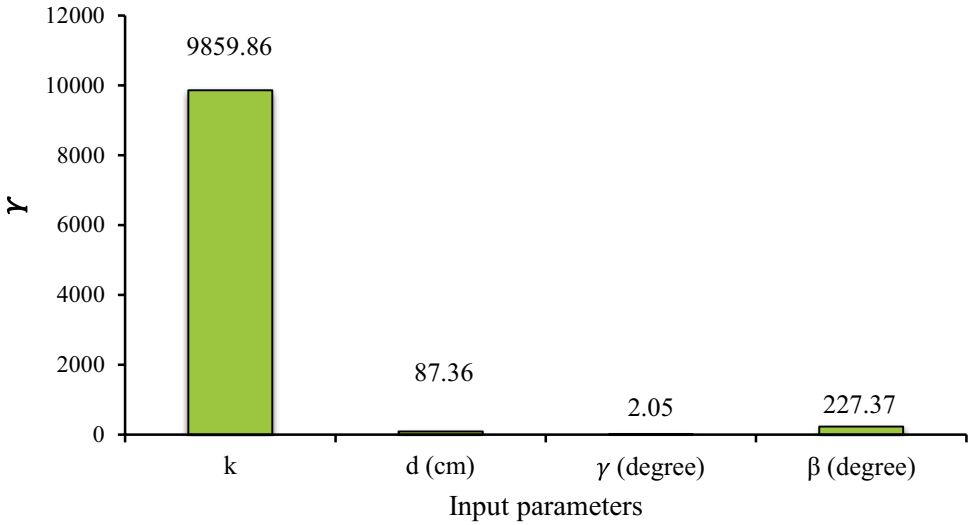


**Fig. 14** Each input parameter's effect on tensile strength

parameter. The following criteria for model parameter sensitivity have been offered based on the ϒ index:

Figure 14 shows the evaluated ϒ index for the $\sigma_t$ model. Tensile strength is quite sensitive to k and $\beta$, but not so much to $d$ and $\gamma$ (see Fig. 14).

## Conclusion

In this paper, diametral loading was applied to a number of Brazilian concrete disc samples containing a set of open non-persistent joints to investigate the effect of joint continuity factor, joint spacing, bridge angle, and loading direction on their tensile strength. ANN, ANFIS, and a combination of ANFIS with PSO and GA were used to propose a comprehensive model for the indirect tensile strength of Brazilian discs. To assess the performance of the models, statistical indices such as $R^2$, RMSE, MSE, MAE, VAF, and CE were used. The results are summarized as follows:

1. ANN has high capability to predict tensile strength of non-persistent jointed Brazilian discs. It has the best performance for the test data with $R^2$=0.966, RMSE=0.176, MSE=0.018, MAE=0.108, VAF=84.852, and CE=0.818.
2. The test data indicated that ANFIS-GA has priority to ANFIS-PSO to predict tensile strength.
3. The multiple parametric sensitivity analysis (MPSA) revealed that $k$ has the highest impact on the tensile strength and after that the model is highly sensitive to $\beta$.
4. The MPSA analysis also shows that the model is also sensitive to $d$ and $\gamma$ parameters, while the latter has the minimum effect on the model.

However, future work for this study will include extensive numerical study to evaluate the effect of joint parameters on the tensile strength and failure pattern of non-persistent jointed Brazilian discs under diametral loading.

## References

Armaghani DJ, Momeni E, Abad SVANK et al (2015) Feasibility of ANFIS model for prediction of ground vibrations resulting from quarry blasting. Environ Earth Sci 74:2845–2860. https://doi.org/10.1007/s12665-015-4305-y

Asadizadeh M, Hossaini MF (2016) Predicting rock mass deformation modulus by artificial intelligence approach based on dilatometer tests. Arab J Geosci 9:96. https://doi.org/10.1007/s12517-015-2189-5

Asadizadeh M, Hossaini MF, Moosavi M et al (2019) Mechanical characterisation of jointed rock-like material with non-persistent rough joints subjected to uniaxial compression. Eng Geol 260:105224. https://doi.org/10.1016/j.enggeo.2019.105224

Asadizadeh M, Majdi A (2019) Developing new Adaptive Neuro-Fuzzy Inference Systems to predict granular soil groutability. International J Mining Geo-Eng 53:133–142. https://doi.org/10.22059/IJMGE.2018.255209.594728

Asadizadeh M, Moosavi M, Hossaini MF (2018a) Investigation of mechanical behaviour of non-persistent jointed blocks under uniaxial compression. Geomech Eng 14:29–42. https://doi.org/10.12989/gae.2018a.14.1.029

Asadizadeh M, Moosavi M, Hossaini MF, Masoumi H (2018b) Shear Strength and Cracking Process of Non-persistent Jointed Rocks: An Extensive Experimental Investigation. Rock Mech Rock Eng 51:415–428. https://doi.org/10.1007/s00603-017-1328-6

Asadizadeh M, Tavakoli H, Rahmannejad R, Mehinrad A (2010) Effect of anisotropy and confining pressure ratio on rock mass deformation modulus at Bakhtiary dam site (Iran). In: ISRM International Symposium - 6th Asian Rock Mechanics Symposium, ARMS 2010. Int Soc Rock Mech Rock Eng

Aydin M, Karakuzu C, Uçar M et al (2013) Prediction of surface roughness and cutting zone temperature in dry turning processes of AISI304 stainless steel using ANFIS with PSO learning. Int J Adv Manuf Tech 67:957–967. https://doi.org/10.1007/s00170-012-4540-2

Azarfar B, Peik B, Abbasi B, Roghanchi P (2018) A discussion on numerical modeling of fault for large open pit mines. 52nd US Rock Mech/Geomech Symp

Bahaaddini M, Hagan P, Mitra R, Hebblewhite BK (2016) Numerical Study of the Mechanical Behavior of Nonpersistent Jointed Rock Masses. Int J Geomech 16:4015035. https://doi.org/10.1061/(ASCE)GM.1943-5622.0000510

Bahaaddini M, Sharrock G, Hebblewhite BK (2013) Numerical investigation of the effect of joint geometrical parameters on the mechanical properties of a non-persistent jointed rock mass under uniaxial compression. Comput Geotech 49:206–225. https://doi.org/10.1016/j.compgeo.2012.10.012

Barton N (1973) Review of a new shear-strength criterion for rock joints. Eng Geol 7:287–332. https://doi.org/10.1016/0013-7952(73)90013-6

Bieniawski ZT, Hawkes I (1978) Suggested Methods for Determining Tensile Strength of Rock Materials. Int J Rock Mech Min Sci 15:99–103

Brady BHG, Brown ET (2004) Rock Mechanics for underground mining. Springer, Netherlands, Dordrecht

Cheng C, Chen X, Zhang S (2016) Multi-peak deformation behavior of jointed rock mass under uniaxial compression: Insight from particle flow modeling. Eng Geol 213:25–45. https://doi.org/10.1016/j.enggeo.2016.08.010

Correa JM, Farret FA, Popov VA, Simoes MG (2005) Sensitivity Analysis of the Modeling Parameters Used in Simulation of Proton Exchange Membrane Fuel Cells. IEEE Trans Energy Convers 20:211–218. https://doi.org/10.1109/TEC.2004.842382

Feng P, Dai F, Liu Y et al (2018) Effects of strain rate on the mechanical and fracturing behaviors of rock-like specimens containing two unparallel fissures under uniaxial compression. Soil Dyn Earthq Eng 110:195–211. https://doi.org/10.1016/j.soildyn.2018.03.026

Haeri H, Sarfarazi V, Zhu Z (2016) Analysis of Crack Coalescence in Concrete Using Neural Networks. Strength Mater 48:850–861. https://doi.org/10.1007/s11223-017-9831-2

Hajihassani M, Jahed Armaghani D, Monjezi M et al (2015) Blast-induced air and ground vibration prediction: a particle swarm optimization-based artificial neural network approach. Environ Earth Sci 74:2799–2817. https://doi.org/10.1007/s12665-015-4274-1

Höglund H (2017) Tax payment default prediction using genetic algorithm-based variable selection. Expert Syst Appl 88:368–375. https://doi.org/10.1016/j.eswa.2017.07.027

Holland JH (1992) Adaptation in Natural and Artificial Systems. The MIT Press

Huang J, Asteris PG, Manafi Khajeh Pasha S et al (2020) A new auto-tuning model for predicting the rock fragmentation: a cat swarm optimization algorithm. Eng Comput. https://doi.org/10.1007/s00366-020-01207-4

Jang J-S (1993) ANFIS: adaptive-network-based fuzzy inference system. IEEE Trans Syst Man Cybern 23:665–685

Jennings JE (1970) A mathematical theory for the calculation of the stability of open cast mines. In: Symp. on Theor. Background to the Plann. of Open Pit Mines. A. A. Balkema, Johannesburg

Karimi J, Asadizadeh M, Hossaini MF et al (2021) Compressive strength of flawed cylindrical specimens subjected to axial loading. Geomech Eng 27:87–99. https://doi.org/10.12989/gae.2021.27.1.087

Lajtai EZ (1973) Fracture From Compressive Stress. Int 7 Rock .tlech Attn Sci & G¢omech Abslr 10:265–284

Lawal AI, Kwon S (2021) Application of artificial intelligence to rock mechanics: An overview. J Rock Mech Geotech Eng 13:248–266. https://doi.org/10.1016/j.jrmge.2020.05.010

Lin Q, Cao P, Meng J et al (2020) Strength and failure characteristics of jointed rock mass with double circular holes under uniaxial compression: Insights from discrete element method modelling. Theoret Appl Fract Mech 109:102692. https://doi.org/10.1016/j.tafmec.2020.102692

Luo Z, Bui X-N, Nguyen H, Moayedi H (2021) A novel artificial intelligence technique for analyzing slope stability using PSO-CA model. Eng Comput 37:533–544. https://doi.org/10.1007/s00366-019-00839-5

Mahmoodzadeh A, Mohammadi M, Ibrahim HH et al (2021) Tunnel geomechanical parameters prediction using Gaussian process regression. Mach Learn App 3:100020. https://doi.org/10.1016/j.mlwa.2021.100020

Martin A, Gayathri V, Saranya G et al (2011) A Hybrid Model for Bankruptcy prediction Using Genetic Algorithm, Fuzzy C-Means and Mars. Int J Soft Comput 2:12–24. https://doi.org/10.5121/ijsc.2011.2102

Momeni E, Nazir R, Jahed Armaghani D, Maizir H (2014) Prediction of pile bearing capacity using a hybrid genetic algorithm-based ANN. Measurement 57:122–131. https://doi.org/10.1016/j.measurement.2014.08.007

Nguyen HQ, Ly H-B, Tran VQ et al (2020) Optimization of Artificial Intelligence System by Evolutionary Algorithm for Prediction of Axial Capacity of Rectangular Concrete Filled Steel Tubes under Compression. Materials 13:1205. https://doi.org/10.3390/ma13051205

Rajabi M, Rahmannejad R, Rezaei M, Ganjalipour K (2017) Evaluation of the maximum horizontal displacement around the power station caverns using artificial neural network. Tunn Undergr Space Technol 64:51–60. https://doi.org/10.1016/J.TUST.2017.01.010

Rezaei M (2019) Forecasting the stress concentration coefficient around the mined panel using soft computing methodology. Eng Comput 35:451–466. https://doi.org/10.1007/s00366-018-0608-4

Rezaei M (2017) Feasibility of novel techniques to predict the elastic modulus of rocks based on the laboratory data. Int J Geotech Eng. https://doi.org/10.1080/19386362.2017.1397873

Rezaei M (2016) Development of an intelligent model to estimate the height of caving–fracturing zone over the longwall gobs. Neural Comput Appl. https://doi.org/10.1007/s00521-016-2809-3

Rezaei M, Asadizadeh M (2020) Journal of Mining and Environment (JME) Predicting Unconfined Compressive Strength of Intact Rock Using New Hybrid Intelligent Models. J Min Environ 11:231–246. https://doi.org/10.22044/jme.2019.8839.1774

Rivera JI, Bonilla CA (2020) Predicting soil aggregate stability using readily available soil properties and machine learning techniques. CATENA 187:104408. https://doi.org/10.1016/j.catena.2019.104408

Saberi H, Sharbati R, Farzanegan B (2022) A gradient ascent algorithm based on possibilistic fuzzy C-Means for clustering noisy data. Expert Syst Appl 191:116153. https://doi.org/10.1016/J.ESWA.2021.116153

Sarfarazi V, Hajiloo M, Ghalam EZ, Ebneabbasi P (2020) Study of tensile behavior of Y shape non-persistent joint using experimental test and numerical simulation. Comput Concr 26:565–576. https://doi.org/10.12989/cac.2020.26.6.565

Shakeri J, Asadizadeh M, Babanouri N et al (2022) The evolution of dynamic energy during drop hammer testing of Brazilian disk with non-persistent joints: An extensive experimental investigation. Theoret Appl Fract Mech 117:103162. https://doi.org/10.1016/j.tafmec.2021.103162

Shang J, West LJ, Hencher SR, Zhao Z (2018) Tensile strength of large-scale incipient rock joints: a laboratory investigation. Acta Geotech 13:869–886. https://doi.org/10.1007/s11440-017-0620-7

Sharbati R, Amindavar H, Sharbati R et al (2022) Optimized Cauchy-Gaussian Blend Model for Stochastic-Parametric Simulation of Seismic Ground Motions. Prevention and Treatment of Natural Disasters 1:38–49. https://doi.org/10.54963/PTND.V1I1.62

Shojaeian A, Asadizadeh M (2020) Prediction of surface tension of the binary mixtures containing ionic liquid using heuristic approaches; an input parameters investigation. J Mol Liq 298:111976. https://doi.org/10.1016/j.molliq.2019.111976

Tsuruta R, Utsuki S, Nakaya M (2019) Development of a System for Automatic Evaluation of the Geological Conditions of Tunnel

Faces Using Artificial Intelligence and Application to a Construction Site. IAEG/AEG Annual Meeting Proceedings, San Francisco, California, 2018 -, vol 4. Springer International Publishing, Cham, pp 49–55

Vaziri MR, Tavakoli H, Bahaaddini M (2022) Statistical analysis on the mechanical behaviour of non-persistent jointed rock masses using combined DEM and DFN. Bull Eng Geol Env 81:177. https://doi.org/10.1007/s10064-022-02674-3

Victoire TAA, Jeyakumar AE (2004) Hybrid PSO–SQP for economic dispatch with valve-point effect. Electr Power Syst Res 71:51–59. https://doi.org/10.1016/j.epsr.2003.12.017

Wang T-T, Huang T-H (2009) A constitutive model for the deformation of a rock mass containing sets of ubiquitous joints. Int J Rock Mech Min Sci 46:521–530. https://doi.org/10.1016/j.ijrmms.2008.09.011

Wittke W (2014) Rock Mechanics Based on an Anisotropic Jointed Rock Model. Wilhelm Ernst & Sohn, Berlin

Yang S-Q, Chen M, Huang Y-H et al (2020) An experimental study on fracture evolution mechanism of a non-persistent jointed rock mass with various anchorage effects by DSCM, AE and X-ray CT observations. Int J Rock Mech Min Sci 134:104469. https://doi.org/10.1016/j.ijrmms.2020.104469

Yang XX, Kulatilake PHSW, Chen X et al (2016) Particle Flow Modeling of Rock Blocks with Nonpersistent Open Joints under Uniaxial Compression. Int J Geomech 16:04016020. https://doi.org/10.1061/(ASCE)GM.1943-5622.0000649